Dalton Transactions

Accepted Manuscript

This is an *Accepted Manuscript*, which has been through the RSC Publishing peer review process and has been accepted for publication.

Accepted Manuscripts are published online shortly after acceptance, which is prior to technical editing, formatting and proof reading. This free service from RSC Publishing allows authors to make their results available to the community, in citable form, before publication of the edited article. This *Accepted Manuscript* will be replaced by the edited and formatted *Advance Article* as soon as this is available.

To cite this manuscript please use its permanent Digital Object Identifier (DOI®), which is identical for all formats of publication.

More information about *Accepted Manuscripts* can be found in the **Information for Authors**.

Doping Potassium Ions in Silver Cyanide Complexes for Green Luminescence†

Xi Liu,[*] Lin Li, Yun-Zhi Yang, and Kun-Lin Huang

ABSTRACT: Doping potassium ions in silver cyanide complexes lead to two heterometallic silver-potassium cyanide complexes, namely, $[Me_4N]_2[KAg_3(CN)_6]$ (**1**) with a typical NaCl-type framework containing distinct ligand-unsupported *argentophilic* interactions, $[Ag_3(H_2O)_3][K(CN)_2]_3$ (**2**) with an unprecedented 3-D (4, 4, 6, 6)-connected framework formed by unique $[Ag_3(H_2O)_3]$ clusters connecting concave-convex $_\infty^2[K(CN)_2]$ layers. The two complexes exhibit green luminescence, and the relationships between their structures and photoluminescence, as well as the regulating effect on the luminescence by doping of potassium ions were well investigated via density functional theory analysis.

Introduction

For several decades, transition metal cyanide complexes have attracted great research interest due to not only their structural diversities with novel topologies, but also their special chemical and physical properties as well as their potential applications in molecule based magnets,[1] electrical conductivity,[2] luminescent materials,[3] etc.[4] Among these functional complexes, silver cyanide complexes have been explored extensively over years on account of their various topologies as well as argentophilic interactions within their structures.[5,6] However, the fascinating photoluminescence of silver cyanide complexes was reported only sporadically,[7,8] and there is still a long way to go about such systems.[9]

[*] *Key Laboratory of Green Synthesis and Applications, College of Chemistry, Chongqing Normal University, Chongqing 401331, P. R. China. E-mail: xliu@cqnu.edu.cn. Tel: +86-023-65910306; Fax: +86-023-65362777*

According to others'[7] and our[8,10] recent studies, silver cyanide complexes possess structural priority as luminescence materials since they consist of silver cations with $4d^{10}$ electronic configuration and linear cyanide groups with delocalized π electron systems. On the one hand, the cations with d^{10} electronic configurations[11] generally have remarkable photophysical and photochemical characteristics, so most of their complexes may emit intense and long-lived luminescence with emission energies spanning a wide range in the visible spectrum when they are coordinated by suitable bridging and ancillary ligands. On the other hand, the bridging ligands with extended π electron systems[8,10] are usually endowed with good potential ability to enhance photoelectron transfer and nonlinear optical reactivity. Furthermore, our previous emission mechanisms studies of silver cyanide complexes with efficient luminescence[8] present that the ancillary ligands (such as halide ions, 2.2'-bipyridine ligand.) have great effects on the energy levels of silver ground state and excitation states, resulting in changing the luminescence lifetimes and quantum yields of the target complexes. However, the regulating effect on the luminescence of silver cyanide complexes by doping of metal ions remains unexplored in the literature. Motivated by this idea, potassium ions were introduced purposefully to the synthetic processes of silver cyanide complexes, and resulted in two novel heterometallic silver-potassium cyanide complexes, namely, $[Me_4N]_2[KAg_3(CN)_6]$ (**1**) with a typical NaCl-type framework containing distinct ligand-unsupported *argentophilic* interactions, $[Ag_3(H_2O)_3][K(CN)_2]_3$ (**2**) with an unprecedented 3-D (4, 4, 6, 6)-connected framework formed by unique $[Ag_3(H_2O)_3]$ clusters connecting concave-convex $_\infty^2[K(CN)_2]$ layers. Their structures, photoluminescence, the relationships between the structures and photoluminescence, as well as the regulating effect on the luminescence by doping of potassium ions were well explored via density functional theory analysis.

Experimental section

Materials and instrumentation

All chemicals except tetrahydrofurnan (THF) solvent was obtained from commercial sources and used without further purification. THF solvent was purified and distilled by conventional methods, and stored under nitrogen before use. Elemental analyses were performed on a Vario

EL III elemental analyzer. The FT-IR spectra were obtained on a Perkin Elmer Spectrum using KBr discs in the range 4000–400 cm^{-1}. Photoluminescence analyses were performed on an Edinburgh FLS920 fluorescence spectrometer, the lifetimes of the emission bands were measured on an Edinburgh LifeSpec-ps system. Thermogravimetric analyses were carried out on a NETZSCH STA 449C unit at a heating rate of 10 °C/min under a nitrogen atmosphere.

Preparation of [Me$_4$N]$_2$[KAg$_3$(CN)$_6$] (1)

A mixture of KAg(CN)$_2$ (199 mg, 1 mmol) and Me$_4$NBr (103 mg, 0.67 mmol) in 10 mL of dry and distilled THF solvent was sealed into a 25 mL polytetrafluoroethylene-lined stainless steel container under autogenous pressure and heated at 100 °C for 3 days, The resultant solution was filtered off into a small tube, which was loaded into a large vial containing 5 mL diethyl ether. The large vial was sealed and left undisturbed at room temperature, and colorless crystals of **1** were collected in ca. 40% yield (based on silver) in one week. Anal. calcd. for **1** (%), C$_{14}$H$_{24}$Ag$_3$KN$_8$: C, 25.21; H, 3.63; N, 16.80. Found: C, 25.16; H, 3.58; N, 16.45. FT-IR (KBr, cm^{-1}): 2890(m), 2821(w), 2743(w), 2707(w), 2146(m), 1978(w), 1476(m), 1455(m), 1433(w), 1352(m), 1284(m), 1249(m), 1108(vs), 1055(w), 961(s), 841(s), 527(m). v (CN): 2146(m).

Preparation of [Ag$_3$(H$_2$O)$_3$][K(CN)$_2$]$_3$ (2)

A mixture of KAg(CN)$_2$ (199 mg, 1 mmol) and Et$_4$NBr (141 mg, 0.67 mmol) in 10 mL of acetonitrile (CH$_3$CN) solvent was sealed into a 25 mL polytetrafluoroethylene-lined stainless steel container under autogenous pressure and heated at 120 °C for 3 days, The resultant solution was filtered off into a small tube, which was loaded into a large vial containing 5 mL diethyl ether. The large vial was sealed and left undisturbed at room temperature, and colorless crystals of **2** were collected in ca. 25% yield (based on silver) in one week. Anal. calcd. for **2** (%), C$_2$H$_2$AgKN$_2$O: C,11.07; H, 0.93; N, 12.91. Found: C, 11.15; H, 1.02; N, 12.89. FT-IR (KBr, cm^{-1}): 3433(br, m), 2983(w), 2523(w), 2133(s), 1631(m), 1479(m), 1434(w), 1388(m), 1364(w), 1170(m), 1053(w), 996(m), 784(m). v (CN): 2133(s).

Single crystal structure determination

Single crystals of **1**, and **2** were mounted on a Rigaku Mercury CCD diffractometer equipped with a graphite-monochromated MoKα radiation (λ = 0.71073 Å) at 293 K. The intensity data sets were collected with ω scan technique and reduced by CrystalClear software.[12] The

structures were solved by the direct methods and refined by full-matrix least-squares techniques. Non-hydrogen atoms were located by difference Fourier map and subjected to anisotropic refinement. Hydrogen atoms were added according to the theoretical models. All of the calculations were performed by Siemens SHELXTL^{TM} version 5 package of crystallographic software.[13] Crystallographic data and structural refinements and the selected bond distances and angles for the presented two complexes are summarized in Table 1 and Table 2 respectively. The Ueq values of C11 and C12 atoms in complex **1** are somewhat larger as compared to that of their neighbor N atom, which can be ascribe to slight disorder of C11 and C12 atoms since they occupy the terminal sites of the isolated $[Me_4N]^+$ cation. Since the C and N atoms in the bridging CN^- groups cannot distinguished crystallographically,[14] assignments based on the refinement of their anisotropic thermal parameters have been made in **1** and **2**. More details on the crystallographic studies as well as atom displacement parameters are given as Supporting Information.

Results and discussion

Synthesis

Both complexes were synthesized via similar reactants ($KAg(CN)_2$ and quaternary ammonium bromide (Me_4NBr or Et_4NBr) in 3 : 2 molar ratio) while in different organic solvents and under different temperatures. When the reactants react in dry and distilled THF solvent, the KBr byproduct is segregated from the reaction system due to its insolubilities in anhydrous THF solvent, resulted in obtaining **1** with its components K^+, Ag^+, CN^- in 1 : 3 : 6 molar ratio; while when the reactants react in CH_3CN solvent, the expectant KBr co-product remains in the reaction system due to the trace water in untreated CH_3CN solvent (AR, 99%), and resulted in yielding **2** with coordinated water molecules. Complex **2** can also be regarded as the recrystallization product of $KAg(CN)_2$ in CH_3CN solvent since the Et_4NBr reactant do not take part in the synthesis reaction directly. It should be noted, the water content in untreated CH_3CN solvent plays an important role in synthesizing **2**, too much (water content > 5%) or less (water content < 0.01%) water content in the reaction system will not lead to **2**.

Crystal structure description of 1

The structure of **1** crystallizes in the trigonal space group *R*-3*c* and features a NaCl-type structure containing distinct ligand-unsupported *argentophilic* interactions. The crystallographically asymmetric unit contains one sixth unique potassium cation, one half silver cation, one cyanide group and one third $[Me_4N]^+$ cation. As shown in Fig. 1, the K1 cation is in an octahedral coordination environment and coordinated by six N atoms from six cyanide groups; while Ag1 cation is approximately linearly connected by two cyanide C atoms to form a subunit of $[Ag(CN)_2]^-$ with the C–Ag–C bond angle of 166.8(2) °. Among the adjacent three $[Ag(CN)_2]^-$ subunits, the average Ag···Ag distance is 3.2008(9) Å, which is shorter than the sum of *Van der Waals* radii for silver (3.44 Å). And along these Ag···Ag vectors, there is no Coulombic interaction[15] or evident ligand-packing effects,[16] such as hydrogen-bonding and π-stacking interactions, suggesting the existence of ligand-unsupported *argentophilic* interactions in **1**. The cyanide groups bridge the potassium and silver cations in μ_2 mode to form a complex 3-D framework, which can be simplified as a highly distorted simple cubic structure with the α-Po topology if the potassium cations are regarded as six-connected nodes while the $[Ag(CN)_2]^-$ subunits are counted as linear linkers (Fig. S1, ESI†). Interestingly, if the adjacent three silver cations with ligand-unsupported *argentophilic* interactions in **1** are considered as another type of six-connected nodes, and cyanide groups are regarded as linear linkers, the framework of **1** exhibits a typical NaCl-type structue, and the $[Me_4N]^+$ cations locate in the cavities of the topological net (Fig. 2).

Crystal structure description of 2

The structure of **2** features an unprecedented 3-D (4, 4, 6, 6)-connected framework formed by unique $[Ag_3(H_2O)_3]$ clusters connecting concave-convex $_\infty^2[K(CN)_2]$ layers. As shown in Fig. 3, there are one silver cation and two potassium cations in the repeating unit. The Ag1 cation locates in a distorted tetrahedral geometry and is coordinated by two C atoms from two μ_4-cyanide groups and two water molecules. Three adjacent silver cations with C_3 symmetry are bridged by three waters to form a unique planar 6-membered $[Ag_3(H_2O)_3]$ cluster, which remains unknown in the literature. Both K1 and K2 cations locate in slightly distorted octahedral coordination geometries and are coordinated by six N atoms from six μ_4-κN:κN:κN:κC-cyanide groups. Within the KN_6 coordination octahedra, the K-N bond distances vary from 2.820(5) to 2.903(5) Å, and the adjacent N-K-N bond angles range

between 83.5(1) to 96.5(1) °. The μ_4-cyanide groups bridge the two kind potassium cations through their N terminal to form a 2-D concave-convex $^\infty_2[K(CN)_2]$ layer (Fig. S2), which can also be regarded as the form of KN_6 coordination octahedra by edge-sharing (Fig. 4). The planar $[Ag_3(H_2O)_3]$ clusters connect the $^\infty_2[K(CN)_2]$ layers through C terminal of μ_4-cyanide groups to form a complex 3-D (4, 4, 6, 6)-connected framework (Fig. 5). If the K1 and K2 cations are considered as 6-connected nodes, Ag1 cations and μ_4-cyanide groups are taken as 4-connected nodes, the framework has the total point symbol of $\{3 \cdot 5^4 \cdot 8\}_3 \{4^3 \cdot 5 \cdot 7^2\}_6 \{4^6 \cdot 5^3 \cdot 6^3 \cdot 7^3\}_2 \{4^6 \cdot 6^6 \cdot 8^3\}$, which represents a new topology analyzed by the TOPOS 4.0 program.[16] This new topology can be evolved as the known (4, 6, 6, 6)-connected net with the total point symbol of $\{4^4 \cdot 6^2\}_6 \{4^6 \cdot 6^6 \cdot 8^3\} \{4^6 \cdot 8^6 \cdot 10^3\} \{4^9 \cdot 6^6\}_2$, when the $[Ag_3(H_2O)_3]$ clusters are regarded as 6-connected nodes.

Photoluminescent properties

Complex **1** exhibits a very strong and sharp green emission band in the solid-state at 490 nm upon maximum photo-excitation at 267 nm, while complex **2** displays two strong fluorescent emission bands in the solid-state at 375 and 530 nm upon maximum photo-excitation at 314 nm (Fig. 6), and their lifetimes were measured to be 2.4 *ns* of 490 nm peak for **1,** 1.3 *ns* of 375 nm peak and 2.6 *ns* of 530 nm peak for **2**.

Density functional theory (DFT) calculation of the electronic band structures of the present two complexes along with density of states (DOS) was carried out with the CASTEP code (Fig. S3 and S4 and their explanations, ESI†),[17,18] which uses one of the three nonlocal gradient corrected exchange-correlation functionals (GGA-PBE). As shown in Fig. 7, for complexes **1**, the top of valence bands (VBs) are mostly formed by the hybridizations of Ag-4d state (35.1 electrons/eV) and Cyanide-2p states (50.4 electrons/eV), in which Ag-4d state peak locates around -1.7 eV and Cyanide-2p states peak settle around -2.4 eV, and the two peaks have a small deviation of 0.7 eV. The bottom of conduction bands (CBs) are mainly contributed from the Cyanide-2p states (23.2 electrons/eV). Accordingly, the origin of the emission band of **1** may be mainly ascribed to the coupling of metal-to-ligand charge transfer (MLCT) and ligand-to-ligand charge transfer (LLCT). For MLCT, the electrons are transferred from the silver (Ag-4d state, VBs) to the unoccupied π^* orbitals of cyanide groups (Cyanide-2p states, CBs), while for LLCT, the electrons are transferred from the occupied π

orbitals of cyanide groups (cyanide-2p states, VBs) to the unoccupied π^* orbitals of cyanide groups (Cyanide-2p states, CBs).

For complex **2** (Fig. 8), the top of VBs are mostly formed by the mixture of Ag-4d state (19.5 electrons/eV) and Cyanide-2p states (24.9 electrons/eV), in which Ag-4d state peak locates around -3.4 eV and Cyanide-2p states peak settle around -4.6 eV, and the two peaks have a large deviation of 1.2 eV, indicating Ag-4d state and Cyanide-2p states have poor hybridizations. The bottom of CBs are mainly contributed from the Cyanide-2p states (13.2 electrons/eV). Accordingly, the origin of the high-energy emission band at 375 nm of **2** may be mainly assigned to ligand-to-ligand charge transfer (LLCT) where the electrons are transferred from the occupied π orbitals of cyanide groups (Cyanide-2p states, VBs) to the unoccupied π^* orbitals of cyanide groups (Cyanide-2p states, CBs), while the origin of the low-energy emission band at 530 nm of **2** may be mainly allocated to metal-to-ligand charge transfer (MLCT) where the electrons are transferred from the silver (Ag-4d state, VBs) to the unoccupied π^* orbitals of cyanide groups (Cyanide-2p states, CBs).

It should be noted, although the top of VBs and the bottom of CBs of complexes **1** and **2** have similar components, complex **1** exhibit one emission peak while complex **2** exhibit two emission peaks, which may be ascribed to the different hybridization extent of Ag-4d state and Cyanide-2p states in the top of VBs. Comparing with complex **1**, the additional coordination of O_{water} to silver cations weakens the covalent bond between the silver cations and cyanide group in **2**, which may not only lead to the poor hybridization and the large deviation between Ag-4d state and Cyanide-2p states in the top of VBs, but also cause the decrease of the unoccupied π^* orbitals energy level of cyanide groups (Fig.7 and Fig. 8). Accordingly, the emission originating from MLCT of **2** exhibits a red shift of 40 nm comparing with that of **1**, while the maximum excitation wavelength of **2** displays an increase of 47 nm comparing with that of **1**.

Furthermore, in the two complexes, the K-4s,4p states have no devotion to the top of VBs while a little contribution to the bottom of CBs, so the emission mechanism of these two heterometallic complexes are comparable to those of our reported homometallic silver cyanide complexes.[8] On the other hand, the K-4s,4p states have large contribution to the bottom of VBs (see ESI†), which may affect the relative energy levels of frontier orbitals and

band-gap energy of complexes as compared to those of our reported homometallic silver cyanide complexes. Accordingly, the doping of alkali potassium ions in silver cyanide complexes has almost no effect on the emission mechanism of the complexes,[8] but that may regulate emission wavelengths of the complexes.

Thermal stability

Compounds **1** and **2** are stable in air, and can maintain their crystallinity at room temperature for several days. The TGA curves show that compounds **1**, **2** decompose at the decomposition point T_{onset} of about 230, 425ºC (Fig. S5 and S6, ESI†), respectively, indicating they are stable materials for practical application. Together with the efficient luminescent properties, the present two compounds are good candidates as luminescent materials. The detailed decomposition mechanisms of the two compounds are too complex to explain at present.

Conclusions

In summary, two heterometallic silver-potassium cyanide complexes with green luminescence were synthesized, and the relationships between their structures and photoluminescence were well explored via DFT analysis. In the two complexes, the doping of alkali potassium ions has almost no effect on the emission mechanism, but that may regulate emission wavelengths as compared to the homometallic silver cyanide complexes. Further experiments based on the doping of transition metal cations in silver cyanide complexes are undergoing. Investigations of the luminescence behaviors of these doping materials will be helpful for the design and synthesis of more efficient luminescent materials.

Acknowledgements

Dalton Transactions Accepted Manuscript

References

1. For reviews, see (a) J. Cernak, M. I. P. Orendac, J. Chomic, A. Orendacova, J. Skorsepa and A. Feher, *Coord. Chem. Rev.*, 2002, **224**, 51–66; (b) R. Lescouezec, L. M. Toma, J. Vaissermann, M. Verdaguer, F. S. Delgado, C. Ruiz-Perez, F. Lloret and M. Julve, *Coord. Chem. Rev.*, 2005, **249**, 2691–2729; (c) H. L. Sun, Z. M. Wang and S. Gao, *Coord. Chem. Rev.*, 2010, **254**, 1081–1100.

2. (a) J. L. Boyer, M. Ramesh, H. J. Yao, T. B. Rauchfuss and S. R. Wilson, *J. Am. Chem. Soc.*, 2007, **129**, 1931–1936; (b) T. Yoshimura, T. Ikai, T. Takayama, T. Sekine, Y. Kino and A. Shinohara, *Inorg. Chem.*, 2010, **49**, 5876–5882; (c) W. Imhof, A. Sterzik, S. Krieck, M. Schwierz, T. Hoffeld, E. T. Spielberg, W. Plass and N. Patmore, *Dalton Trans.*, 2010, **39**, 6249–6254; (d) X. D. Zheng, Y. L. Hua, R. G. Xiong, J. Z. Ge and T. B. Lu, *Cryst. Growth Des.*, 2011, **11**, 302–310.

3. (a) R. C. Evans, P. Douglas and C. J. Winscom, *Coord. Chem. Rev.*, 2006, **250**, 2093–2126; (b) Y. Y. Lin, S.W. Lai, C.M. Che, W. F. Fu, Z. Y. Zhou and N. Y. Zhu, *Inorg. Chem.*, 2005, **44**, 1511–1524; (c) Y.-L. Qin, J.-J. Hou, J. Lv and X.-M. Zhang, *Cryst. Growth Des.*, 2011, **11**, 3101–3108; (d) A. N. Ley, L. E. Dunaway, T. P. Brewster, M. D. Dembo, T. D. Harris, F. Baril-Robert, X. Li, H. H. Patterson and R. D. Pike, *Chem. Commun.*, 2010, **46**, 4565–4567; (e) E. Chelebaeva, J. Larionova, Y. Guari, R. A. S. Ferreira, L. D. Carlos, F. A. Almeida Paz, A. Trifonov and C. Guerin, *Inorg. Chem.*, 2009, **48**, 5983–5995; (f) E. Chelebaeva, J. Larionova, Y. Guari, R. A. S. Ferreira, L. D. Carlos and F. A. A. Paz, *Inorg. Chem.*, 2008, **47**, 775–777; (g) B. A. Maynard, R. E. Sykora, J. T.Mague and A. E. V. Gorden, *Chem.Commun.*, 2010, **46**, 4944–4946; (h) F. Jin, Y. Zhang, H.-Z.Wang, H.-Z. Zhu, Y. Yan, J. Zhang, and J.-Y. Wu, *Cryst. Growth Des.*, 2013, **13**, 1978−1987.

4. (a) K. W. Chapman, P. D. Southon, C. L. Weeks, and C. J. Kepert, *Chem. Commun.* 2005, 3322–3324; (b) A. L. Goodwin, D. A. Keen, M. G. Tucker, M. T. Dove, L. Peters and J. S. O. Evans, *J. Am. Chem. Soc.*, 2008, **130**, 9660–9661; (c) A. Deak, T. Tunyogi and G. Palinkas, *J. Am. Chem. Soc.*, 2009, **131**, 2815–2816; (d) S. I. Nishikiori, H. Yoshikawa, Y. Sano and T. Iwamoto, *Acc. Chem. Res.*, 2005, **38**, 227–234; (e) S. S. Kaye, H. J. Choi, and J. R. Long, *J. Am. Chem. Soc.*, 2008, **130**, 16921–16925; (f) P. D. Southon, L. Liu, E. A. Fellows, D. J. Price, G. J. Halder, K. W. Chapman, B. Moubaraki, K. S. Murray, J. F. Letard and C. J. Kepert, *J. Am. Chem. Soc.*, 2009, **131**, 10998–11009; (g) A. L. Goodwin, M. Calleja, M. J. Conterio, M. T. Dove, J. S. O. Evans, D. A. Keen, L. Peters and M. G. Tucker, *Science*, 2008, **319**, 794–797; (h) A. E. Phillips, A. L. Goodwin, G. J. Halder, P. D. Southon and C. J. Kepert, *Angew. Chem., Int. Ed.*, 2008, **47**, 1396–1399.

5. For ligand-supported *argentophilic* interactions, see: (a) G.-C. Guo, G.-D. Zhou, Q.-G. Wang, and T. C. W. Mak, *Angew. Chem., Int. Ed. Engl.*, 1998, **37**, 630–632; (b) G.-C. Guo, and T. C. W. Mak, *Angew. Chem., Int. Ed. Engl.*, 1998, **37**, 3183–3186; (c) G.-C. Guo, G.-D. Zhou, and T. C. W. Mak, *J. Am. Chem. Soc.*, 1999, **121**, 3136–3141; (d) Q.-M. Wang, and T. C. W. Mak, *J. Am. Chem. Soc.*, 2001, **123**, 7594–7600; (e) Q.-M. Wang, and T. C. W. Mak, *Inorg. Chem.*, 2003, **42**, 1637–1643.

6. For ligand-unsupported *argentophilic* interactions, see: (a) Y. Kim, and K. J. Seff, *J. Am. Chem. Soc.*, 1978, **100**, 175–180; (b) K. Singh, J. R. Long, and P. Stavropoulos, *J. Am. Chem. Soc.*, 1997, **119**, 2942–2943; (c) M. A. Omary, T. R. Webb, Z. Assefa, G. E. Shankle, and G. E. Patterson, *Inorg. Chem.*, 1998, **37**, 1380–1386; (d) M. L. Tong, X. M. Chen, B. H. Ye, and L. N. Ji, *Angew. Chem., Int. Ed.*, 1999, **38**, 2237–2240; (e) O. Kristiansson, *Inorg. Chem.*, 2001, **40**, 5058–5059; (f) G. A. Bowmaker, Effendy, P. C. Junk, B. W. Skelton, and A. H. White, *Z. Naturforsch.*, 2004, **59b**, 1277–1292.

7. (a) Y. Lin, S. Lai, and C. Che, *Inorg. Chem.*, 2005, **44**, 1511–1524; (b) J. Lin, Z. Li, J. Li, and S. Du, *Polyhedron*, 2007, **26**, 107–114; (c) Y. Ling, F.-P. Zhai, M.-L. Deng, D. Wu, Z.-X. Chen, X.-F. Liu,

Y.-M. Zhou, and L.-H. Weng, *CrystEngComm*, 2012, **14**, 1425–1431.

8. (a) X. Liu, G.-C. Guo, M.-L. Fu, W.-T. Chen, M.-S. Wang, and J.-S. Huang, *Inorg. Chem.*, 2006, **45**, 3679–3685; (b) X. Liu, G.-C. Guo, M.-L. Fu, W.-T. Chen, J.-Z. Zhang, and J.-S. Huang, *Dalton Trans.*, 2006, 884–886.

9. (a) C. A. Bayse, J. L. Ming, K. M. Miller, S. M. McCollough, and R. D. Pike, *Inorg. Chim. Acta*, 2011, **375**, 47–52; (b) A. M. Chippindale, S. J. Hibble, E. J. Bilbé, E. Marelli, A. C. Hannon, C. Allain, R. Pansu, and F. Hartl, *J. Am. Chem. Soc.*, 2012, **134**, 16387−16400.

10. (a) X. Liu, G.-C. Guo, A.-Q. Wu, L.-Z. Cai, and J.-S. Huang, *Inorg. Chem.*, 2005, **44**, 4282–4286; (b) X. Liu, G.-C. Guo, M.-L. Fu, J.-P. Zou, F.-Q. Zheng, and J.-S. Huang, *Inorg. Chim. Acta*, 2006, **359**, 1643–1649; (c) X. Liu and G.-C. Guo, *Cryst. Growth Des.*, 2008, **8**, 776–778; (d) X. Liu and G.-C. Guo, *Aust. J. Chem.*, 2008, **61**, 481–483; (e) X. Liu, K.-N. Zhao, G. Xu, and G.-C. Guo, *Chinese J. Struct. Chem.*, 2010, **29**, 1524–1528; (f) X. Liu, K.-L. Huang, G.-M. Liang, M.-S. Wang, and G.-C. Guo, *CrystEngComm*, 2009, **11**, 1615–1620; (g) X. Liu and K.-L. Huang, *Inorg. Chem.* 2009, **48**, 8653–8655.

11. V. W.-W. Yam and K. K.-W. Lo, *Chem. Soc. Rev.* 1999, **28**, 323–334.

12. Rigaku, CrystalClear Version 1.35; Rigaku Corporation, 2002.

13. Siemens, SHELXTL^{TM} Version 5 Reference Manual, Siemens Energy & Automation Inc.; Madison, Wisconsin, USA, 1994.

14. J. C. Dyason, P. C. Healy, L. M. Engelhardt, C. Pakawatchai, V. A. Patrick, and A. H. White, *J. Chem. Soc., Dalton Trans.*, 1985, 839–844.

15. G. A. Bowmaker, R. K. Harris, B. Assadollahzadeh, D. C. Apperley, P. Hodgkinson, and P. Amornsakchai, *Magn. Reson. Chem.* 2004, **42**, 819–826.

16. V. A. Blatov, *Struct. Chem.*, 2012*, **23***, 955–963.

17. (a) M. Segall, P. Linda, M. Probert, C. Pickard, P. Hasnip, S. Clark and M. Payne, *Materials Studio CASTEP*, version 5.5; Accelrys: San Diego, CA, 2010. (b) M. Segall, P. Linda, M. Probert, C. Pickard, P. Hasnip, S. Clark and M. Payne, *J. Phys.: Condens. Matter*, 2002, **14**, 2717–2744.

18. For examples, see (a) Y. Zhang, W. Cheng, D. Wu, H. Zhang, D. Chen, Y. Gong, and Z. Kan, *Chem. Mater.* 2004**, 16***, 4150–4159; (b) Z. Fang, W. Yang, J. He, K. Ding, X. Wu, Q. Zhang, R. Yu, and C. Lu, *CrystEngComm*, 2012, **14**, 4794–4800.
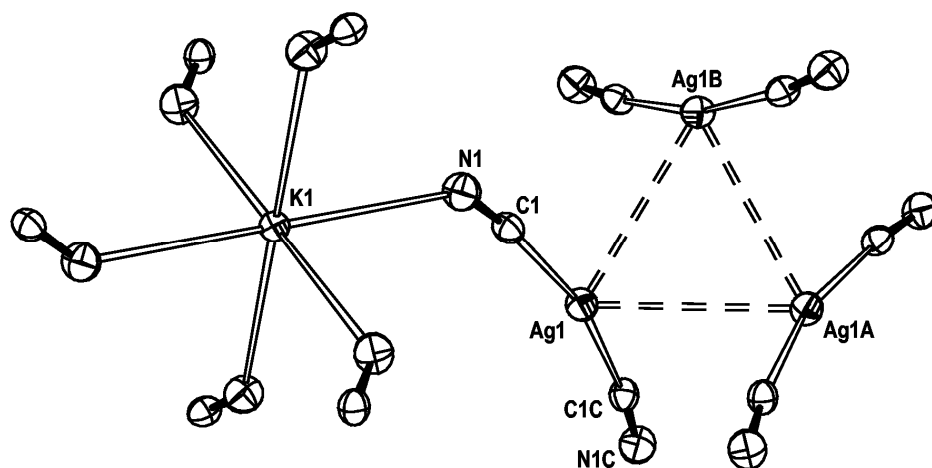
Fig. 1 The coordination environments of silver and potassium cations in **1** with 30% thermal ellipsoids**.** The silver-silver interaction is represented as double dashed lines. Symmetry codes A: -x+*y*, -1-*x*, *z*; B: -1-*y*, -1+*x*-*y*, *z*; C: 1/3+*y*, -1/3+*x*, 1/6-*z*.
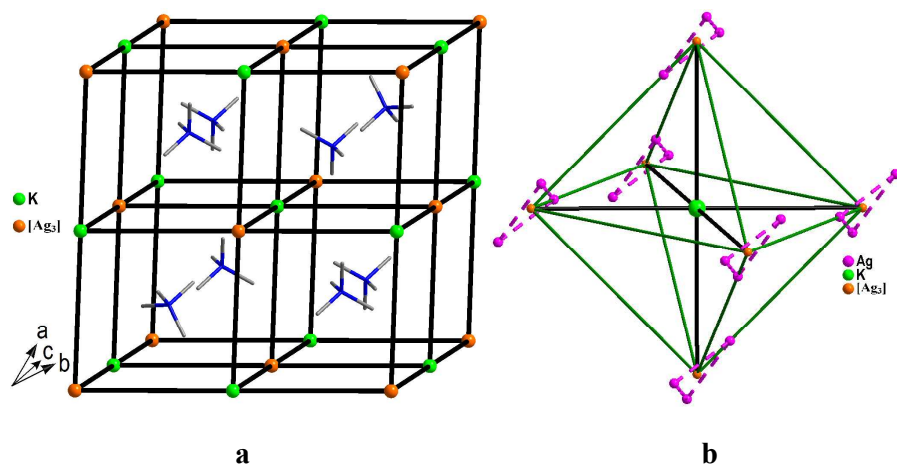

Fig. 2 The packing diagram of **1** with typical NaCl-type topology (a), and the relative positions of the silver and potassium cations in **1** (b). The orange balls represent the centers of the adjacent three silver cations with ligand-unsupported *argentophilic* interactions.
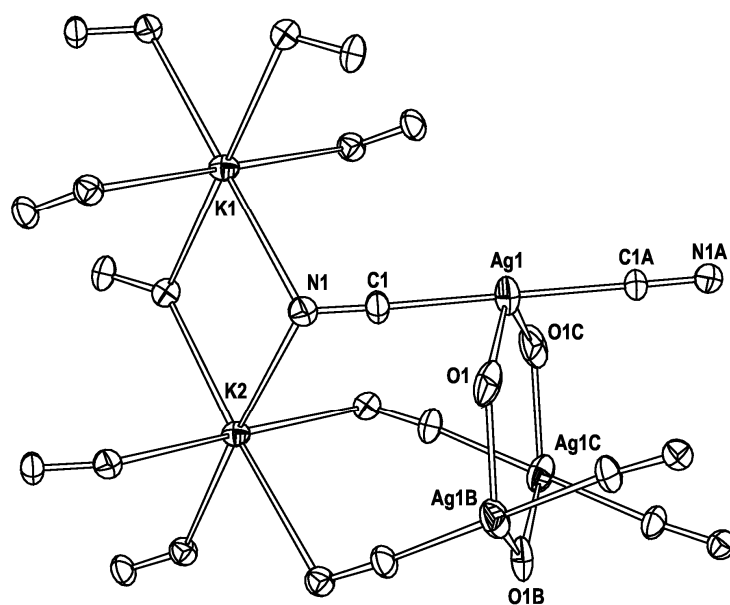
Fig. 3 The coordination environments of silver and potassium cations in **2** with 30% thermal ellipsoids. Symmetry codes A: *x*, 1+*x*-*y*, 3/2-*z*; B: 1-*y*, 1+*x*-*y*, *z*; C: -*x*+*y*, 1-*x*, *z*.
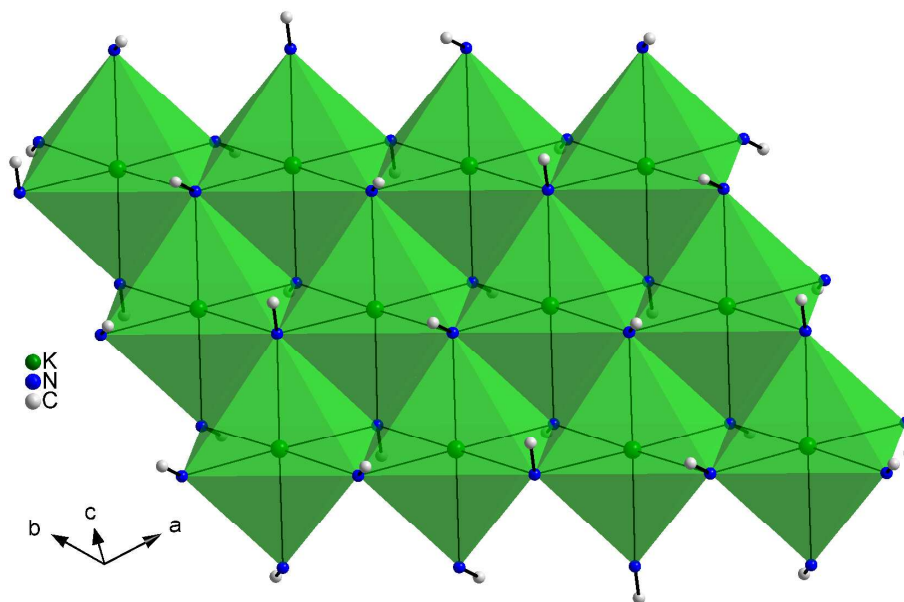

Fig. 4 A view of 2-D concave-convex $^{\infty}_{2}[K(CN)_2]$ layer in **2** formed by edge-sharing of KN_6 octahedra.
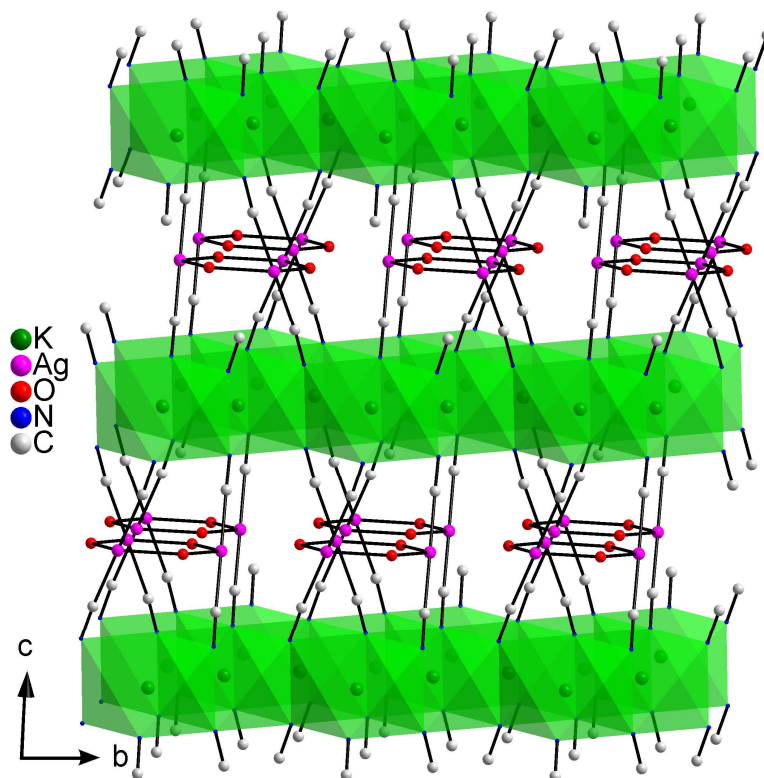
Fig. 5 The $[Ag_3(H_2O)_3]$ clusters connect the $_\infty^2[K(CN)_2]$ layers to form a 3-D framework. The hydrogen atoms are omitted for clarity.
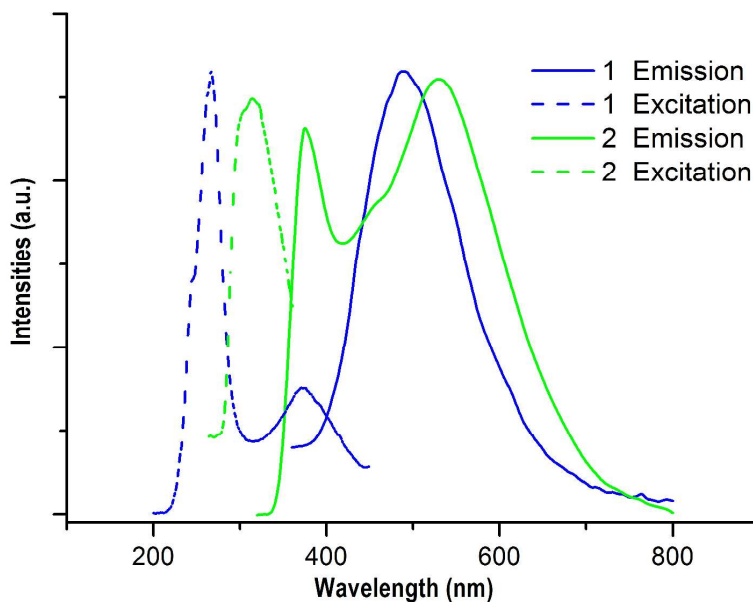

Fig. 6 Solid-state electronic emission spectra of **1** (λ_{ex} = 267 nm) and **2** (λ_{ex} = 314 nm) at room temperature.
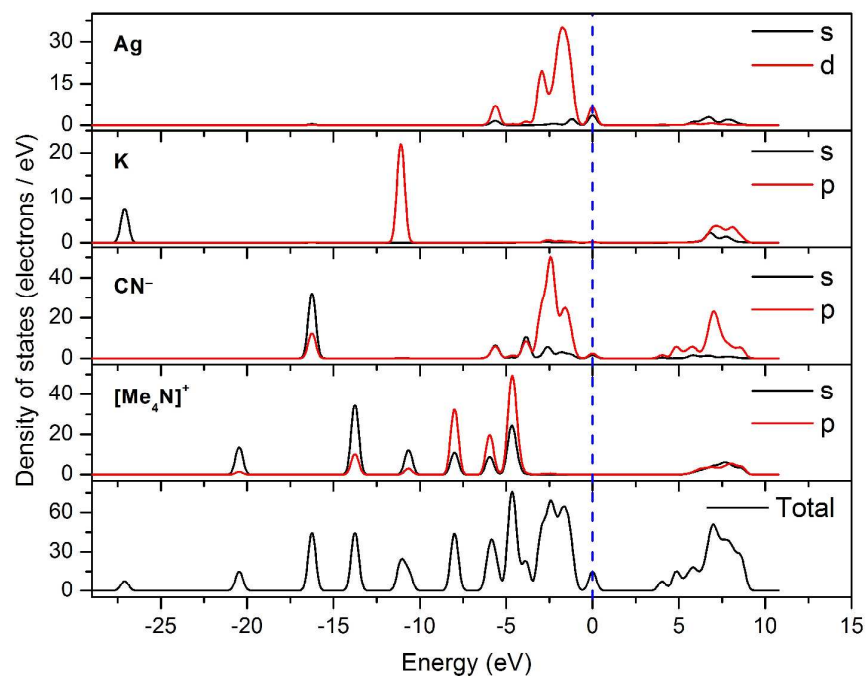
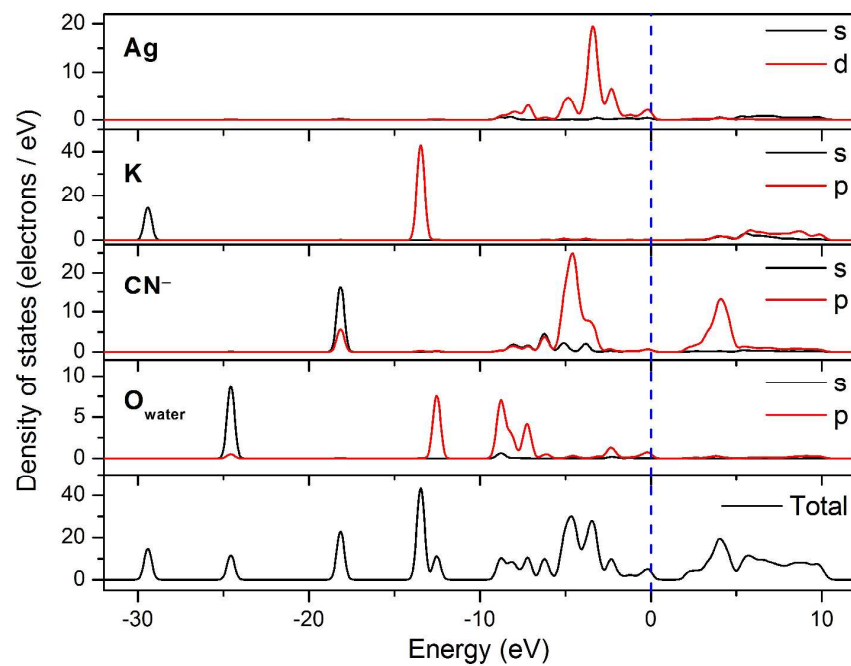**Fig. 7** The total and partial density of states of **1**. The Fermi level is set at 0 eV.

Fig. 8 The total and partial density of states of **2**. The Fermi level is set at 0 eV.

Table 1. Crystal Data and Structure Refinements for **1-2**.

Complex	1	2
Formula	$C_{14}H_{24}Ag_3KN_8$	$C_2H_2AgKN_2O$
T (K)	293(2)	293(2)
Molecular weight	667.12	217.03
Crystal Size (mm^3)	$0.22 \times 0.20 \times 0.20$	$0.50 \times 0.30 \times 0.22$
Crystal system	Tigonal	Trigonal
Space group	R-$3c$	P-$31c$
a (Å)	9.2899(10)	7.3932(8)
b (Å)	9.2899(10)	7.3932(8)
c (Å)	49.248(3)	17.641(3)
α (°)	90	90
β (°)	90	90
γ (°)	120	120
V ($Å^3$)	3680.8(6)	835.06(18)
D_{calc} (Mg m^{-3})	1.806	2.589
Z	6	6
F (000)	1944	612
Absorption coefficient (mm^{-1})	2.553	4.244
Reflections collected/unique (R_{int})	8826/944 (0.0401)	4852/506 (0.0356)
Data /parameters/restraints	661/41/0	385/34/0
R^a	0.0359	0.0465
$R_w{}^b$	0.0707	0.1268
Goodness-of-fit on F^2	1.003	1.002
$\Delta\rho_{max}$ and $\Delta\rho_{min}$ (e $Å^{-3}$)	0.461 and -0.373	1.016 and -0.905

^{a} $R = \sum||F_0| - |F_c||/\sum F_0$. ^{b} $R_w = \{[\sum(F_0^2 - F_c^2)^2/[\sum w(F_0^2)^2]\}^{1/2}$.

**Table 2** Selected Bond Lengths (Å) and Bond Angles (°) for **1-2**.

Bond	Dist.(Å)	Angel	(°)
1			
Ag1-C1	2.078(5)	C1C-Ag1-C1	166.8(2)
Ag1-Ag1A	3.2008(9)	C1-Ag1-Ag1A	114.8(1)
Ag1-Ag1B	3.2008(9)	C1-Ag1-Ag1B	77.2(1)
K1-N1	2.950(5)	Ag1A-Ag1-Ag1B	60.0
C1-N1	1.093(5)	N1-C1-Ag1	173.3(4)
		C1-N1-K1	138.9(4)
2			
K1-N1	2.863(4)	N1-C1-Ag1	174.5(6)
K1-N1D	2.863(4)	C1-Ag1-C1A	179.7(3)

15

K2-N1	2.903(5)	C1-Ag1-O1C	110.67(19)
K2-N1E	2.820(5)	C1-Ag1-O1	69.19(19)
Ag1-C1	2.053(6)	O1C-Ag1-O1	117.2(3)
Ag1-O1	2.084(3)	Ag1B-O1-Ag1	122.8(3)
N1-C1	1.151(7)	C1-N1-K1	110.7(4)
Ag1-O1C	2.084(3)	C1-N1-K2	110.5(4)

Symmetry codes: for **1**: A: -x+y, -1-x, z; B: -1-y, -1+x-y, z; C: 1/3+y, -1/3+x, 1/6-z; for **2**: A: x,

1+x-y, 3/2-z; B: 1-y, 1+x-y, z; C: -x+y, 1-x, z; D: y, 1-x+y, 1-z; E: -1+y, -x+y, 1-z.

16

Graphical Abstract
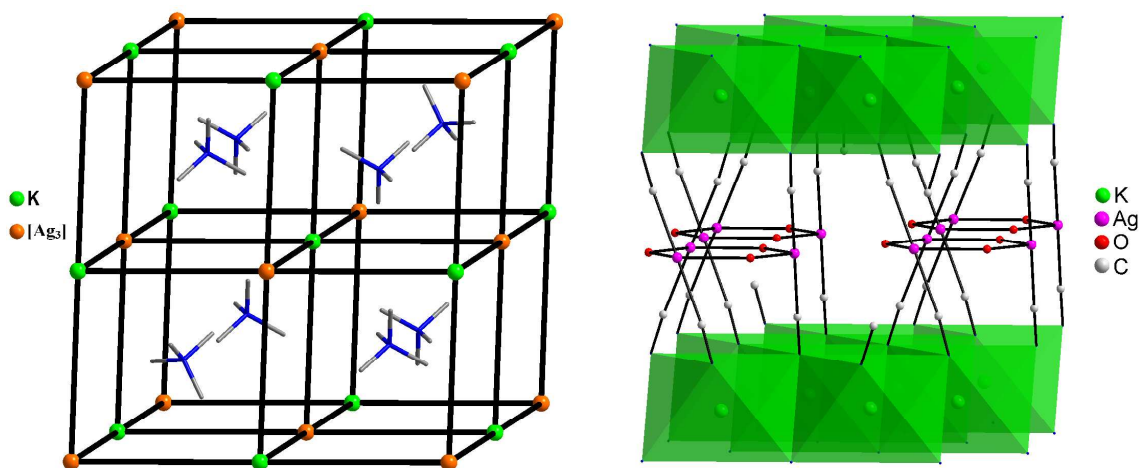
Two heterometallic silver-potassium cyanide complexes are synthesized via solvothermal reactions and diffusion processes, which exhibit green luminescence.